

Electrochemical Synthesis of MoO₃ Nanoparticles Effect of Temperature Convert to MoO₃ Nanorods

N. R. Dighore, S. P. Jadhav, S. T. Gaikwad, A. S. Rajbhoj*

*(Department of Chemistry, Dr. Babasaheb Ambedkar Marathwada, University, Aurangabad-431004, India)

ABSTRACT

MoO₃ nanorods were prepared by electrochemical reduction method using the tetra propyl ammonium bromide (TPAB) was structure directing agent in an organic medium *viz.* tetra hydro furan (THF) and acetonitrile (ACN) in 4:1 ratio and at current density 14mA &18 mA. The reduction process takes place under atmospheric condition over a period of 2 h. Dried sample was calcinated in muffle furnace at 500°C. The parameters such as current density and concentration of stabilizers were used to control the size of nanorods. The synthesized MoO₃ nanorods were characterized by using UV-Visible, FT-IR, XRD, SEM-EDS and TEM analysis techniques.

Keywords – Current density, electrochemical method, MoO₃ nanoparticles, MoO₃ nanorods, tetra propyl ammonium bromide.

I. INTRODUCTION

The electrochemical method for production of nanoparticles has been widely studied since early work of Reetz[1-2]. This indicated that size selective nanosize transition metal particles could be prepared electrochemically using tetraalkylammonium salts as stabilizers of metal cluster in a nonaqueous medium. The electrochemical method has been demonstrated to superior to other nanoparticles synthesis methods because lower processing temperature, simple equipment set up, low cost and high yield & purity of nanoparticles.

In recent years much effort has been devoted to the study of molybdenum oxides & related materials. Molybdenum oxide existence of several different allotropes & sub-oxides phases [3], such as MoO₂ (monoclinic), MoO₄ (monoclinic, orthorhombic), Mo₈O₂₄ (monoclinic), Mo₉O₂₆ (triclinic, monoclinic) and two polytypic phases for MoO₃. One is the thermodynamic stable orthorhombic MoO₃ (α -MoO₃) phase an n-type semiconductor with wide band gap of 3.2 eV [4] and other is the metastable monoclinic MoO₃ (β - MoO₃) phase with ReO₃ type structure [5]. Their properties strongly change as a function of oxygen vacancy concentration & nonstoichiometry.

Molybdenum oxide is a potential material because of its wide range of stoichiometry and interesting behavior which includes structural[6], chemical[7], electrical and optical[8] properties. MoO₃ is an attractive example of a prospective electrode material for Li-batteries[9] with high capacity & has been evaluated as both cathode[10] and anode[11] materials. It exhibits a unique layer structure, which permits lithium ion intercalation/deintercalation [12-14]. As a wide band gap n type semiconducting materials, MoO₃ has

received considerable attention in many technological applications such as erasable optical storage media, optical switching coatings and high density memory devices, gas & chemical sensors[15-16] catalysis[17-18] photography, future display materials[19-20], energy efficient window technology[5], photochromic & electrochromic devices[21] and so many.

Recently there have been number of process developed to synthesize MoO₃ nanocrystals with controlled shape and size[8], such as nanobelts[5], nanoribbons[22], nanorods[23], nanofibers [24] nanoplatelets/nanosheets[25], nanowires[26], nanoflakes[27] and nanotubes[28] which have been successfully prepared using various technologies including hydrothermal, sol gel, thermal evaporation and electrochemical processes. Nanowires & nanorods are typically cylindrical, hexagonal, square or triangular in cross section. In this article nanorods are typically rectangular in cross section with high anisotropic dimensions and controlled crystal size which could be achieved by varying current density & temperature.

II. EXPERIMENTAL

2.1 Materials

Tetra propyl ammonium bromide (TPAB) (A.R.), tetrahydrofuran (THF) and acetonitrile (ACN) were purchased from Aldrich and S.D. Fine chemicals and used as such. The sacrificial anode in the form of molybdenum sheet and platinum sheet as inert cathode having thickness 0.25 mm and purity 99.9% were purchased from Alfa Aesar. The specially designed electrolysis cell with a volume of 30ml was used.

2.2 Synthesis of MoO₃ Nanoparticles & MoO₃ nanorod

In electrochemical reduction method for oxidation of bulk metal and reduction of metal ions for size selective preparation of tetra propyl ammonium salt stabilized metal nanoparticles. In the initial experiment we have used a molybdenum metal sheet (1x1 cm) as anode and a platinum sheet (1x1 cm) as the cathode. These two electrodes were placed parallel to one another and were separated by 1.0cm in 0.01 M solutions of TPAB prepared in ACN/THF (4:1) which also served as the supporting electrolyte (scheme-1). The electrolysis process was then carried out at two different current densities 14 mA/cm² & 18 mA/cm² for 2.0 hrs. For UV-visible spectroscopic study, 2.0 ml of the sample solution was withdrawn after completion of electrolysis process and solution was allowed to settle for one day. The agglomerated solid sample was separated from the solution by decantation and washed three to four times with THF. The washed samples were then dried under vacuum desiccator and store in air tight containers. As obtained MoO₃-TPAB crystallite compound was used as precursor to prepare MoO₃ nanorods. The dried sample of MoO₃-TPAB crystallite compound was placed in a silica crucible which was then put into the electric muffle furnace and kept at 500°C temperature for 2 hours. After natural cooling down to room temperature gave bright pale yellowish crystals of molybdenum oxide nanorods were obtained.

2.3 Characterization of Nanoparticles

The prepared molybdenum oxide nanorods were characterized by UV-Visible, FT-IR, XRD, TEM, SEM-EDS techniques. The UV-Visible spectrum was recorded on spectrophotometer [JASCO 503] with a quartz cuvette using ACN / THF (4:1) as reference solvent. The IR spectra were recorded on FT-IR spectrophotometer [JASCO FT-IR/4100] Japan using dry KBr as standard reference in the range of 400–4000 cm⁻¹. The X-ray powder diffraction patterns of the molybdenum oxide nanorods were recorded on Bruker 8D advanced X-ray diffractometer using CuK α radiation of wavelength = 1.54056 Å. To study the morphology and elemental composition, molybdenum oxide nanorods were examined using SEM and energy dispersive spectrophotometer (EDS), The SEM analysis were carried out with JEOL; JSM- 6330 LA operated at 20.0kV and 1.0000nA. Shape, size and morphology calculated by TEM analysis was carried out with Philips model CM200 operated at 200kv.

III. RESULTS AND DISCUSSION

3.1 UV-visible Spectroscopy

The UV-visible absorption spectrum recorded for molybdenum oxide nanoparticles a shown in Fig 3.1a & 3.1b exhibits maximum absorption at 634nm &

642nm for TPAB at 14mA and TPAB at 18 mA respectively. The metal nanoparticles exhibit absorption bands or broad regions of absorption in the UV-visible range due to the excitation of surface plasmon resonances (SPR) or interband transitions; these SPR are characteristic properties for the metallic nature of particles. The prominent peak observed at 634nm & 642 nm, in the visible wavelength, is due to the absorption of surface Plasmon. This absorption band can be attributed to the surface Plasmon resonance (SPR) peak of molybdenum oxide nanoparticles. Red shift from 634 to 642 was observed as the particle size decreased because of increase in intensity of absorption peaks and current density respectively. A broad peak around 634nm & 642nm can be attributed to wide size distribution of particles form in the solution. The particles showed hardly any change in the absorption spectra even after a month of ageing time indicating highly stable nature of particles. The broadening of SPR peak was due to the agglomeration of the nanoparticles in the sample and high width of these particles distribution.

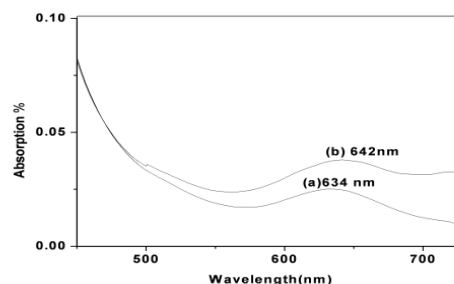


Fig. 3.1 UV-visible spectra of molybdenum crystals capped with TPAB of 0.01 M solution at (a) 14mA & (b) 18mA current density

3.2 FT-IR Spectroscopy

In IR Spectrum of molybdenum oxide nanoparticles shown in fig. 3.2a & 3.2b, broad peaks appear at 3432 cm⁻¹ & 1633 cm⁻¹ due to the stretching and bending vibration of hydroxyl groups adsorbed on molybdenum oxide nanoparticles. The peak at 949 cm⁻¹ is due to the terminal Mo=O bond which indicate the layered orthorhombic phase[10] and absorption at 848 cm⁻¹ & 597 cm⁻¹ are of the stretching and bending mode of vibration Mo-O-Mo. The spectrum also contains distinct peaks at 496 cm⁻¹ & 669 cm⁻¹, which correspond to the mixed phase that contains molybdenum and molybdenum oxide.

The IR spectra of nanorods obtained after heating at 500°C (fig. 3.2c & 3.2d) show the peak at 989 cm⁻¹ due to the terminal Mo=O bond which indicate the layered orthorhombic MoO₃ phase. Absorption at 848 cm⁻¹ is attribute the stretching vibration of the oxygen atom in the Mo-O-Mo unit and at 580 cm⁻¹ is due to bending mode of the Mo-O-

Mo unit which reveals that the oxygen ion is shared by three molybdenum ions. Absorption of H₂O on the sample take place due to contact of sample with environment which give rise to hydrogen bonding of all surface O-H groups, the broad band around 3424 cm⁻¹ is the stretching mode of vibration O-H groups & 1633 cm⁻¹ can be assigned to the bending mode of O-H groups of absorbed water. Hydrogen bonded O-H groups show (H...O-H) bending vibration at 1420 cm⁻¹ and 2974 cm⁻¹ for O-H stretching.

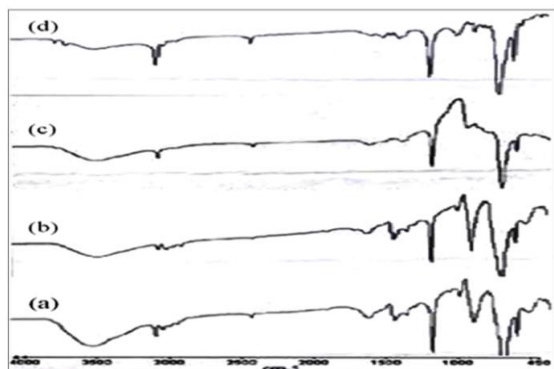


Fig.2 IR spectra of MoO₃ at 14mA & 18 mA current density (a), (b) before heated and (c), (d) heated at 500°C.

3.3 X-Ray diffraction

The X- ray diffraction pattern shown in fig.3.3 explains the crystal structure and phase composition of MoO₃ nanocrystalline materials. The sharp diffraction peaks suggest crystalline nature of nanomaterials. It can be observed in fig. 3.3a & 3.3b that orthorhombic lattice system with lattice parameter a=3.966 Å, b=13.82 Å, c= 3.703Å(JCPDS: 05-0506) and strong peaks at (001) & (011) show crystalline nature of molybdenum oxide nanoparticles. Few peaks of other phase occur due to the impurity. The effect of heating temperature at 500°C as observed in XRD spectrum (fig.3c & 3d) reveals that MoO₃ nanorods have orthorhombic lattice system with lattice parameter a=3.96Å, b= 13.85Å, c=3.696Å,(JCPDS: 35-0609). Interestingly, no peaks of any other phases or impurities were detected, indicating high purity of MoO₃ nanorods. When compared with the standard XRD results, most of the peaks are matched & at (0k0) a strong peak appears for nanorods. Considering these results with regard to the crystal structure of bulk MoO₃ the (010) & (100) planes encloses the nanorods facets along the longitudinal direction & the (001) planes enclose the growth direction (fig. 3.3e). In fig. 3.3c, 3.3d observed that (040), (060) are very strong peaks respectively, that means all the strong diffraction peaks correspond to (0k0) planes compared to the other (hkl) planes of the MoO₃ nanorods indicating the highly anisotropic growth as well as the preferred orientation of the nanorods. In fig. 3.3c & 3.3d (110), (021), (130) & (002) are weak peaks, which show

that crystal growth is slow in these direction, causing decrease in the crystal diffraction line intensity. The surface area to volume ratio of nano-crystals is given by

$$d = \frac{K\lambda}{\beta \cos \theta} \quad (1)$$

Where K known as Scherrer's constant (shape factor), ranging from 0.9 to 1.0, λ=1.5418 is the wavelength of the X-ray radiation source, β is the width of the XRD peak at half height and θ is Bragg angle. The average particle size of the powder was calculated by using Debye-Scherrer formula (1). In Table 3.1(entries a-d) shows the decrease in particle size with increasing current density and also calcinate temperature is given.

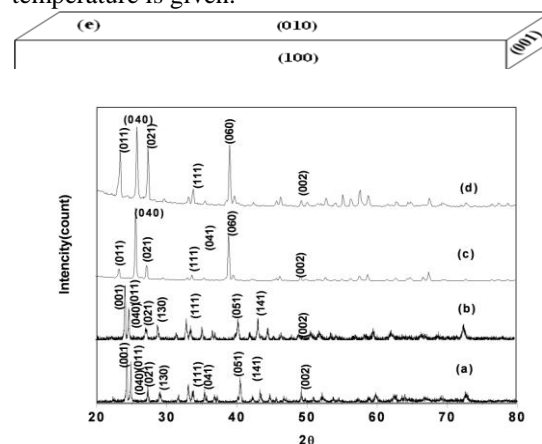


Fig. 3.3 XRD pattern of MoO₃ nanoparticles at 14mA & 18 mA current density (a), (b) before heated, (c), (d) after heated at 500°C and (e) Orientation of nanorod.

From Table 3.1, intense peaks appear at 24.273, 24.246, 25.723 & 25.723 for hkl plane 001, 001, 040 & 040 respectively. The change of current density from 14mA to 18mA decreases the crystalline size from 182.57 nm to 59.41nm. The effect of heating at 500°C also decreases the crystalline size from 40.11nm to 31.44nm.

Table 3.1- Change in particle size with change in current density and calcinations temperature

Entry	MoO ₃ nano	2θ degree	h k l	FWHM	Size (nm)
a	Mo-14 TPAB	24.273	001	0.110	182.57
b	Mo-18 TPAB	24.246	001	0.176	59.41
c	Mo-14 TPAB-500°C	25.723	040	0.236	40.11
d	Mo-18 TPAB-500°C	25.723	040	0.291	31.44

3.4 Scanning Electron Microscopy

The morphology of product were examined by scanning electron microscope. Fig.3.4a & 3.4b reveals sample before calcination ununiform crystals which show with square and cubical like structures. The effect of current density reduces the size of nanomaterials as shown in morphology in fig. 3.4a & 3.4b. The effect of calcining at 500°C changes the morphology from particles to nanorods as shown in fig. 3.4c & 3.4d which show flat or belt like and few cylindrical wire like nanorods of MoO₃. Energy dispersive X-ray spectra were also recorded to determine the chemical composition of MoO₃ nanorods. Result from the EDX spectra show that the nanorods contain only molybdenum and oxygen elements.

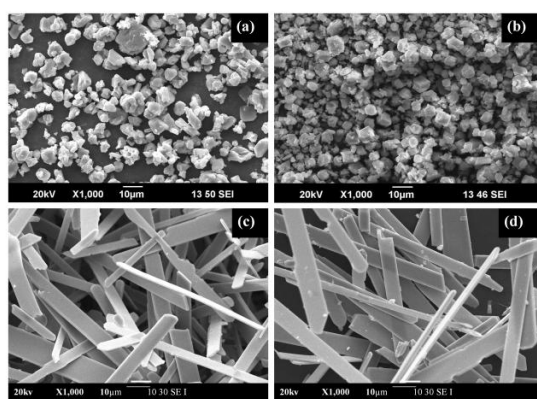


Fig. 3.4 SEM micrograph of MoO₃ nanoparticles at 14mA & 18 mA current density(a), (b) before heated and (c), (d) after heated at 500°C.

3.5 Transmission Electron Microscope

The size and morphology of product were examined by transmission electron microscope (TEM) micrograph of MoO₃ crystal. Before heating (fig. 3.5a & 3.5b) square & few irregular shape crystallites occurred with size of few tens of micron. Fig. 3.5c-f show the effect of heating at 500°C in which change in the morphology from irregular shape to uniform nanorods with 20-120 nm width and length of few tens of micron. In fig. 3.5e & 3.5f cylindrical wire nanorods, mostly flat or belt nanorods were present. The selected area electron diffraction (SAED) pattern recorded perpendicular to the growth axis of individual nanorods could be indexed to the [010] zone axis of diffraction of orthorhombic MoO₃(fig. 3.5g & 3.5h). The spot pattern of SAED confirms that the compounds are single crystalline nanorods.

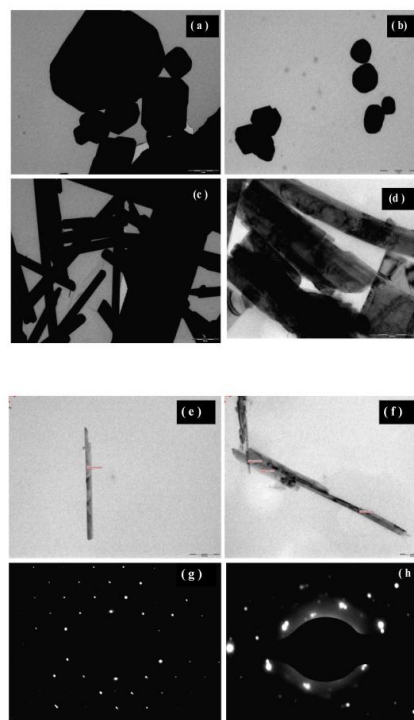


Fig. 3.5 TEM images of MoO₃ nanoparticles at 14 mA & 18 mA current density (a),(b) before heated and (c), (d) after heated at 500°C,(e) cylindrical rod, (e) belt like nanorods & SAED pattern (g) & (h).

IV. CONCLUSIONS

In the present study successfully synthesis of MoO₃ nanocrystalline material by electrochemical method & effect of calcination temperature was studied when change of morphology to nanorods was observed. Also varying the current density from 14mA/cm² to 18mA/cm² the compound reduces size from 182nm to 59nm before calcinations and the size further decreases from 40nm to 30nm after calcination calculated from XRD data. The synthesis of nanorods possesses high crystallinity & narrow size distribution with high anisotropy.

V. ACKNOWLEDGMENT

The authors are grateful do Department of Chemistry, Dr. Babasaheb Ambedkar Marathwada University, Aurangabad and UGC-SAP-DRS-1 scheme New Delhi for providing laboratory facility. One of the author (ASR) thankful for financial assistance from Major Research project [F. No. 832/2010(SR)], University Grants Commission, New Delhi, India.

REFERENCES

- [1] M. T. Reetz, W. Helbig, *Size selective synthesis of nanostructure transition metal clusters*, J Am Chem Soc,116, 1994, 7401-7402.

- [2] M. T. Reetz, W. Helbig, S.A. Quaiser, *Electrochemical preparation of nanostructural bimetallic clusters*, Chem Mater., 7, 1995, 2227-2228.
- [3] V. Bhosle, A. Tiwari, J. Narayan, *Epitaxial growth and properties of MoO_x(2<x<2.75) films*, J Appl Phys.,97, 2005, 83539-1.
- [4] J. W. Rabalais, R. J. Cotton, A. M. Guaman, *Trapped electrons in substoichiometric MoO₃ observed by X-ray electron spectroscopy* Chem Phys Lett., 29, 1974, 131-133.
- [5] L. Zheng, Y. Xu, D. Jin, Y. Xie, *Novel metastable hexagonal MoO₃ nanobelts: synthesis, photocromic and electrochromic properties*, Chem Mater. 21, 2009, 5681-5690.
- [6] D. Parviz, M. Kazemeini, A.M. Rashid, K.J. Jozani, *Synthesis and characterization of MoO₃ nanostructures by solution combustion method employing morphology and size control*, J Nanopart Res. 12, 2010, 1509-1521.
- [7] Y. Shi, B. Guo, S. A. Corr, Q. Shi, Y. S. Hu, K. R. Heier, L. Chen, R. Seshadri, G. D. Stucky, *ordered mesoporous metallic MoO₂ materials with high reversible lithium storage capacity*, Nanolett, 9(12), 2009, 4215-4220.
- [8] Y. Zhao, J. Liu, Y. Zhou, Z. Zhang, Y. Xu, H. Naramoto, S. Yamamoto, *Preparation of MoO₃ nanostructure and their optical properties*, J Phys Cond Matter, 15, 2003, 547-552.
- [9] Y. Xu, X. Cao, Y. Zhang, *Silver nanoparticles modified MoO₃ with enhanced electrochemical properties for Lithium-ion batteries*, Can J Chem. 92, 2014, 16-18.
- [10] L. Mai, B. Hu, W. Chen, Y. Qi, C. Lao, R. Yand, Y. Dai, Z. Wang, *Lithiated MoO₃ nanobelts with greatly improved performance for lithium batteries*, Adv Mater. 19, 2007, 3712-3716.
- [11] N. A. Chernova, M. Roppolo, A. C. Dillon, M. S. Wittingham, *Layered vanadium and molybdenum oxide: batteries and electrochromics*, J Mater Chem. 19, 2009, 2526-2552.
- [12] W. Li, F. Cheng, Z. Tao, J. Vapour transformation preparation and reversible lithium intercalation /deintercalation of α -MoO₃ microrods Chen, J Phys Chem B, 110, 2006, 119-124.
- [13] J. W. Bullard III, R.L. Smith, *Structural evaluation of MoO₃ during lithium intercalation*, Solid State Ionics, 160, 2003, 335-349.
- [14] J. S. Chen, Y. L. Cheah, S. Madhavi, X.W. Lou, *Fast synthesis of α -MoO₃ nanorods with controlled aspects of ratios and their enhance lithium storage capabilities*, J Mater Chem C, 114, 2010, 8675-8678.
- [15] Ganguly, R. George, *Synthesis, characterization and gas sensitivity of MoO₃ nanoparticles*, Bull Mater Sci, 30(2), 2007,183-185.
- [16] D. Chen, *Single-crystalline MoO₃ nanoplates: topochemical synthesis and enhanced ethanol-sensing performance*, J Mater Chem., 21, 2011, 9332-9342.
- [17] F. Wang, W. Ueda, *Nanostructure molybdenum oxide and their catalytic performance in the alkylation of arenes*, ChemComm.2008, doi:10.1039/B803205J.
- [18] F.Wang, W. Ueda, *High catalytic efficiency of molybdenum trioxide in the benzylation of arenes and as investigation of reaction mechanism*, Chem- Eur Journals, 15, 2009, 742-754.
- [19] P. Pichat, M. Mozzanega, C. Hong-Van,) *Room temperature photoassisted formation of hydrogen molybdenum bronzes with alcohol as hydrogen source*, J Phys Chem. 92, 1988,464-467.
- [20] B. R. Faughanan, R.S. Crandall, *Optical properties of mixed oxide WO₃ and MoO₃ electrochromic film*, Appl Phys Latter, 31, 1977, 834-835.
- [21] J. Chen, H. Yang, L. Cheng, *Sonochemical preparation and characterization of photocromic MoO₃ nanoparticles*, Front Phys China, 1, 2007, 92-95.
- [22] L. Cheng, M. W. Shao, X. H. Wang, H. B. Hu, *Single crystalline molybdenum trioxide nanoribbons: photo catalytic, photo conductive and electrochemical properties*, Chem- Eur Journals, 15, 2009, 2310-2316.
- [23] C. V. Reddy, E. H. Walker, S. A. Wicker, Q. L. Williams, R. R. Kallurai, *Characterisation of MoO₃ nanorods for lithium battery using PVP as surfactant J Solid State Electrochem*, 13, 2009, 1945-1949.
- [24] Michallovski, G. R. Patzke, *Hydrothermal synthesis of molybdenum oxide based materials: stategy and structural chemistry*, Chem Eur Journal, 12, 2006, 9122-9134.
- [25] D. Mariotti, H. Lindstrom, A. C. Bose, K. Ostrikov, *Monoclinic β -MoO₃ nanosheet produce by atmospheric microplasma: application to lithium -ion batteries*, Nanotechnology, 19, 2008, 495302.
- [26] M. H. Kim, B. Lee, S. Lee, C. Larson, J.M. Baik, C. T. Yavuz, S. Seifert, S. Vajda, R.E. Winans, M. Moskovits, G. D. Stucky, A. M. Wodtke, *Growth of metal oxide nanowires from supercooled liquid nanodroplets*, Nano Lett., 11, 2009, 4138-4146.
- [27] B. Yan, Z. Zheng, J. Zhang, H. Gong, Z. Shen, W. Huang, T. Yu, *Orientation of controllable growth of MoO₃ nanoflakes: Microraman, field emission and birefringence properties*, J Phy Chem. C, 113, 2009, 20259-20263.
- [28] S. Hu, X. Wang, *Single-walled MoO₃ nanotubes*, J Am Chem Soc.,130, 2008, 8126-8127.